

Evaluation of Thermochemical Models for Particle and Continuum Simulations of Hypersonic Flow

Iain D. Boyd* and Tahir Gökçen*
Eloret Institute, Palo Alto, California 94035

Computations are presented for one-dimensional, strong shock waves that are typical of those that form in front of a re-entering spacecraft. The fluid mechanics and thermochemistry are modeled using two different approaches. The first employs traditional continuum techniques in solving the Navier-Stokes equations. The second approach employs a particle simulation technique, the direct simulation Monte Carlo method (DSMC). The thermochemical models employed in these two techniques are quite different. The present investigation presents an evaluation of thermochemical models for nitrogen under hypersonic flow conditions. Four separate cases are considered that are dominated in turn by vibrational relaxation, weak dissociation, strong dissociation, and weak ionization. In near-continuum, hypersonic flow, the nonequilibrium thermochemical models employed in continuum and particle simulations produce nearly identical solutions. Furthermore, the two approaches are evaluated successfully against available experimental data for weakly and strongly dissociating flows.

Introduction

A SPACE-VEHICLE passing through the Earth's atmosphere will traverse a number of different flow regimes. At lower altitudes, the fluid density is sufficiently large for the flow to be considered in thermochemical equilibrium. However, as the vehicle ascends higher into the atmosphere, the molecular collision rate falls, and low-density effects become increasingly important.

Continuum methods are successfully applied to flows in which the collision rate of the gas is sufficient to maintain Boltzmann energy distributions for the various thermal modes of the gas. It is not necessary that the temperatures associated with each of the different modes be equal, or that chemical equilibrium prevails. Particle methods, such as the direct simulation Monte Carlo method (DSMC), are successfully applied to flows in which a reduced collision rate no longer supports equilibrium energy distributions. As the numerical cost of this technique is proportional to the fluid density, application has mainly been limited to rarefied flows.

The computation of flow properties for the flight trajectories of many space vehicles require the use of both continuum and particle methods mentioned above. The interface between the different flow regimes is therefore of great importance. Clearly, it is desirable to obtain consistent results with these numerical methods in an overlapping near-continuum flow regime. Although the thermochemical models employed in continuum and particle methods are quite different, under conditions of thermochemical equilibrium they are expected to provide identical solutions. The relationship between the continuum and particle simulations under conditions of thermochemical nonequilibrium, however, has not been thoroughly investigated. Therefore, it is the purpose of this article to study this relationship by computing typical hypersonic flows with both the continuum and particle simulation methods.

Evaluation of the thermochemical models is made through the computation of four different cases. The flow conditions

in the studies are given in Table 1 and are chosen to examine the effects of vibrational relaxation, dissociation, and ionization. These processes are considered in an accumulative sense through a gradual increase in the initial enthalpy of the flow. The continuum and particle approaches employed in this work are briefly described below.

Continuum Approach

In the continuum formulation, a nonequilibrium 11-species gas model for air (N_2 , O_2 , NO , N , O , N_2^+ , O_2^+ , NO^+ , N^+ , O^+ , e^-) has been implemented. The thermal state of the gas is described by three temperatures: 1) translational, 2) rotational, and 3) vibrational-electronic. The governing Navier-Stokes equations are supplemented by the equations accounting for thermochemical nonequilibrium processes. The equation set consists of 15 partial differential equations: 11 mass conservation equations for species, one momentum equation for quasi one-dimensional flow, and three energy equations. Since the experimental data is for nitrogen gas, the subset (N_2 , N , N_2^+ , N^+ , e^-) of the air model relevant to the dissociation and ionization of nitrogen is active. The thermochemistry model is basically that proposed by Park.^{1,2} The relaxation time for vibrational-translational energy exchange is taken from Millikan and White³ with Park's modification which accounts for the limiting cross section at high temperatures. Another of Park's modifications concerning the diffusive nature of vibrational relaxation is not included, which is consistent with the current particle model. For vibration-dissociation coupling, the average vibrational energy lost or gained due to dissociation or recombination is taken as 30% of the dissociation energy.¹ The chemical reaction rates are prescribed by Park's model where the basic dissociation rate is assumed to be governed by the geometric average of translational and vibrational temperatures.

The numerical approach to solve the governing equations is fully implicit for fluid dynamics and chemistry. It uses flux vector splitting for convective fluxes and shock capturing. An

Table 1 Flow conditions

Case	U_1 , m/s	ρ_1 , kg/m ³	p_1 , Torr	U_2 , m/s
1	4,000	1.75×10^{-3}	1.17	541
2	4,800	4.67×10^{-2}	31.2	480
3	7,310	7.48×10^{-3}	5.00	496
4	10,000	5.00×10^{-4}	0.33	640

Received April 30, 1992; presented as Paper 92-2454 at the AIAA 27th Thermophysics Conference, Nashville, TN, July 6–8, 1992; revision received Aug. 13, 1992; accepted for publication Aug. 26, 1992. Copyright © 1992 by the American Institute of Aeronautics and Astronautics, Inc. All rights reserved.

*Research Scientist, NASA Ames Research Center, MS 230-2. Member AIAA.

Table 2 Leading constants in chemical rate data, m³/molecule/s

Reaction	Continuum ²	Particle ¹⁹	Particle (present)
1. N ₂ + N ₂ → 2N + N ₂	$1.16 \times 10^{-8} T^{-1.6}$	$6.17 \times 10^{-9} T^{-1.6}$	$7.97 \times 10^{-13} T^{-0.5}$
2. N ₂ + N → 2N + N	$4.98 \times 10^{-8} T^{-1.6}$	$1.85 \times 10^{-8} T^{-1.6}$	$7.14 \times 10^{-8} T^{-1.5}$
3a. N ⁺ + N ₂ → N + N ₂ ⁺	$1.66 \times 10^{-18} T^{0.5}$	$1.67 \times 10^{-17} T^{-0.18}$	$1.66 \times 10^{-18} T^{0.5}$
3b. N + N ₂ ⁺ → N ⁺ + N ₂	See Ref. 1	$2.37 \times 10^{-18} T^{-0.52a}$	$2.34 \times 10^{-14} T^{-0.61}$
4a. N + N → N ₂ ⁺ + e ⁻	$7.31 \times 10^{-23} T^{1.5}$	$2.98 \times 10^{-20} T^{0.77}$	$7.31 \times 10^{-23} T^{1.5}$
4b. N ₂ ⁺ + e ⁻ → N + N	See Ref. 1	$8.88 \times 10^{-10} T^{-1.23}$	$1.57 \times 10^{-17} T^{0.85}$
5. N + e ⁻ → N ⁺ + 2e ⁻	$4.15 \times 10^4 T^{-3.82}$	1.00×10^{-14}	$5.81 \times 10^{-8} T^{-1.0}$

^aSee text for details of an error in this published data.

adaptive grid strategy is also implemented. For the computations in this article, a quasi-one-dimensional code is used and a freestream of pure nitrogen is prescribed. The details of the numerical method can be found in Refs. 4–6.

Particle Approach

The particle simulation code employed in this investigation provides modeling of the translational, rotational, vibrational, and electron kinetic energy distributions. These are complemented through simulation of dissociative, recombinative, ionizing, and exchange reactions. The code is vectorized for efficient execution on a Cray-YMP. Description of the vectorized implementation can be found in Refs. 7 and 8. The boundary conditions employed in the one-dimensional flow are reflecting pistons set to the upstream and downstream velocities. The downstream velocity is obtained either from the continuum calculations, or from available experimental data. The present simulations compute the entire shock structure from upstream to downstream conditions. Once the shock reaches a specified location, small adjustments are made to the coordinate system of the computational grid to maintain a steady shock position.

The rate of energy exchange between the translational and rotational energy modes is simulated using a probability function evaluated using the energy of each collision.⁹ The mechanics of rotational energy exchange is performed by the Borgnakke-Larsen¹⁰ approach. The rate of energy exchange involving the vibrational energy mode is simulated using a high-temperature model.¹¹ The mechanics of vibrational energy exchange are computed using two different schemes. The first uses the Borgnakke-Larsen approach with a continuous vibrational energy distribution described by a fixed number of vibrational degrees of freedom ζ_v . The second approach, due to McDonald,¹² allows sampling of postcollision vibrational energy levels from the discrete form of the simple harmonic oscillator (SHO). This approach does not require the value of ζ_v to be estimated for the whole flowfield. Instead, it effectively varies ζ_v according to the local energy content of the flow, therefore, it is the preferred approach from a physical standpoint. The manner in which the mechanics of energy exchange is performed in the particle simulation is shown by Lumpkin et al.¹³ to affect the rate of relaxation. Therefore, all the rotational and vibrational relaxation models employed in the particle simulations are adjusted to match the continuum values by the correction developed by Ref. 13.

Dissociation reactions are modeled with the vibrationally favored dissociation (VFD) model proposed by Haas and Boyd.¹⁴ As its name suggests, this model includes the important physical phenomenon of vibration-dissociation coupling. The model contains a free parameter ϕ which controls the degree of coupling between vibrational and dissociative relaxation processes. It was demonstrated in Ref. 14 that by increasing the value of ϕ , it is possible to increase the dissociation incubation time in the simulation. Also in Ref. 14, through comparison with experimental data, the value of ϕ for nitrogen was determined assuming Borgnakke-Larsen mechanics for vibrational energy exchange with a fixed value for ζ_v . In the DSMC code, the model employed for the reverse recombination reaction appropriate to VFD is that developed

by Boyd.⁸ All other chemical reactions, i.e., ionization and exchange reactions are simulated using the steric factor developed by Bird.¹⁵ The inclusion of electrons in the simulation is discussed in detail in Ref. 16.

Chemical Rate Coefficients

The rate coefficients employed in the reactions of interest in the present study are given in Table 2. These are described in the usual Arrhenius form

$$k(T) = aT^b \exp(-E_a/kT)$$

where a and b are empirically determined constants, E_a is the activation energy, and T is the controlling temperature. Three different sets of coefficients are given corresponding to those used 1) in the continuum code, 2) in previous DSMC investigations, and 3) in the present DSMC code. The values of the activation energy used in the three sets of rate data are unchanged for each separate reaction. Therefore, the exponential term in the Arrhenius form has been omitted from Table 2.

The rate expressions employed in the continuum code are those recommended in the review by Park et al.² Generally, only the forward rate constants are specified. In the dissociation reactions—reactions 1 and 2—the controlling temperature in the continuum two-temperature approach is given by $T_a = (TT_e)^{1/2}$. For nitrogen dissociation, the particle code employs the rates of Byron¹⁷ in the VFD model. It was previously shown by Boyd⁸ that these rates, when used with the VFD model, are capable of reproducing vibration-dissociation coupling observed at high temperatures.

The reverse rates for each reaction are obtained by evaluating the following temperature-dependent form for the equilibrium constants proposed by Park¹:

$$\ln[K_e(T)] = A_1 z + A_2 + A_3 \ln(z) + A_4/z + A_5/z^2$$

where the A_i are constants and $z = 10,000/T$. In the continuum code, the values of A_i for reaction 3 are obtained from Ref. 18, while those for reaction 4 are taken from Ref. 1. Unfortunately, this form for the equilibrium constant is not mathematically convenient for implementation in the DSMC chemistry models. However, a set of reverse reaction rates for use in DSMC has been determined by Bird,¹⁹ and these have been used in a number of studies. These reverse reaction rates are determined by calculating an equilibrium constant in which the exponential terms in the electronic partition functions are evaluated at a temperature of 11,000 K. It is possible to compute the equilibrium constants employed by Bird by considering the ratio of the forward and reverse rates for each reaction. This has been performed for reactions 3 and 4 of Table 2. The equilibrium constant employed by Bird and that used in the continuum code are shown as a function of temperature for reaction 3 in Fig. 1. It should be noted that the exponential term has again been omitted for the sake of simplicity. For this reaction, it is found that the equilibrium constant employed by Bird is about two orders of magnitude higher than the continuum expression. Review of this article led to the discovery of an error in the reverse reaction rate

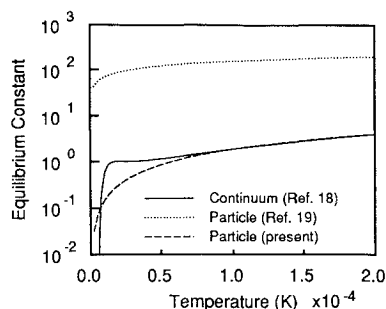


Fig. 1 Variation of the equilibrium constant with temperature for reaction 3.

published in Ref. 19 for reaction 3b. The correct value²⁰ for the temperature exponent should be -0.18 instead of -0.52 . In reaction 4, the equilibrium constant used by Bird gives values which are again generally higher than the continuum model.

It is to be noted that the goal of the present study is to evaluate differences in the chemical models employed in the continuum and particle methods. To limit the number of factors involved in the comparisons, it is our aim to maintain consistency between the relaxation rates employed in the solution techniques. Therefore, a form for the equilibrium constant which takes the traditional Arrhenius form is curve-fitted as a function of temperature to Park's expression. The limitation on the Arrhenius form which may be used conveniently in Bird's expression for the probability of chemical reaction¹⁵ is discussed by Boyd and Stark.²¹ The curve fit for reaction 3 is also shown in Fig. 1. The resulting rate constants for the reverse direction for reactions 3 and 4 are listed in Table 2. Generally, good agreement is obtained between the new DSMC expressions and Park's results, particularly over the temperature range of interest, i.e., from 5000 to 20,000 K.

For reaction 5, the temperature-dependent form proposed in Ref. 2 is not convenient for use in the DSMC chemistry models. In comparing the forward rate constants employed by Park and Bird for this reaction, it is noted that Bird's reaction rates are several orders of magnitude lower. Once again, a curve fit is made to Park's expression in an Arrhenius form which may be employed in the particle chemistry models. The new form, which is given in Table 2, gives closer correspondence to Park's results over the temperature range of interest. Further analyses have been performed which improve the correspondence between the chemical rates employed in continuum and particle simulation for all reactions in air involving charged species, and they are reported in Ref. 16.

Presentation of Results

Computations are performed for four different sets of flow conditions for normal shockwaves in pure nitrogen, and these are listed in Table 1 in which subscripts 1 and 2 indicate upstream and downstream conditions, respectively. The upstream temperature is prescribed to be 300 K for all cases. The upstream density together with the length of the computational domain simulated are chosen such that the flows are in the near-continuum regime. In other words, Knudsen number is small enough that the thickness of the shockwave is small compared to relaxation distance behind the shock. The different upstream flow conditions also provide increasing enthalpy; thus, the flow behind the shock is characterized in case 1 by vibrational relaxation processes, in case 2 by weak dissociation, in case 3 by strong dissociation, and in case 4 by weak ionization. The conditions in cases 2 and 3 correspond to those investigated experimentally by Kewley and Horning.²² The results for each of these investigations are described in the following subsections. The numerical parameters chosen for each DSMC computation followed the usual

guidelines in setting the cell size less than the mean free-path and the time-step to be a fraction of the mean time between collisions. The cell size criterion is relaxed in regions far behind the shock-front where flow gradients are less severe. In each case considered, the number of computational cells is 1000, and the number of simulated particles is maintained at about 100,000.

Case 1: Vibrationally Relaxing Flow

Density profiles for the first case investigated are shown in Fig. 2. Very good agreement is found between the continuum and particle simulation results. Two different DSMC computations are shown; the first corresponds to the use of the Borgnakke-Larsen (BL) approach for performing the mechanics of vibrational energy exchange with a constant number of vibrational degrees of freedom (DOF) $\zeta_v = 1.6$. This value corresponds closely to that evaluated at the downstream equilibrium temperature. The second solution employed the discrete vibrational energy sampling approach for the simple harmonic oscillator (SHO) of McDonald⁷ which automatically varies ζ_v . This is the first time that a comprehensive comparison is made between continuum and particle simulations for vibrational relaxation behind a strong shock. It is very encouraging to observe that, under near-continuum conditions, the two methods give such close agreement.

The variation in translational and vibrational temperatures for this case are shown in Fig. 3. The particle solutions are obtained with McDonald's variable ζ_v model. Once again, very good agreement is obtained between the two solution techniques. Temperature is generally a much more sensitive quantity to simulate than density. The close correspondence between the continuum and particle results indicates that the vibrational relaxation models of both approaches are very nearly equivalent. This comparison, therefore, lends strong support to the use in the particle simulation of the vibrational energy exchange probabilities developed for the DSMC method,¹¹ the correction term required to equate the continuum and particle relaxation rates,¹³ and the mechanics of vibrational energy exchange.¹² It should be noted that the degree of dissociation under these flow conditions is less than 1%.

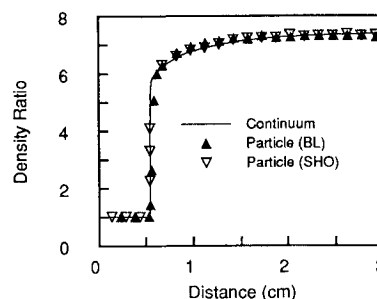


Fig. 2 Comparison of continuum and particle solutions of the local to upstream density ratio for case 1.

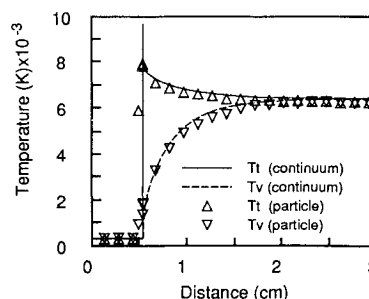


Fig. 3 Comparison of continuum and particle solutions of the translational and vibrational temperatures for case 1.

Case 2: Weakly Dissociating Flow

The second set of conditions considered has an increased enthalpy which gives rise to weak dissociation behind the shock. This case is of additional interest, as it was studied experimentally by Kewley and Hornung²² who employed interferograms to measure the variation in density behind strong shocks of nitrogen. The increase in enthalpy is revealed in the density profiles shown in Fig. 4 in which the normalized density rise reaches a value of about 10 at the downstream boundary. While both solutions give good agreement with the experimental data, it is clear that the particle solution provides the better correspondence. The DSMC profile is obtained with the variable ζ_v model. Comparison of the translational and vibrational temperatures computed through the shock are shown in Fig. 5. Again, a very good agreement is observed for the two sets of results. Considering the excellent agreement obtained in Fig. 5 between the continuum and particle methods, and also for the case of vibrational relaxation, it is concluded that the differences observed in Fig. 4 must be due to the dissociation models employed in each simulation technique. This indicates that the continuum two-temperature model gives a dissociation rate which is slightly slower than that of experiment and DSMC. In other words, for a weakly dissociating gas, the effect of vibrational relaxation on dissociation is overestimated in Park's two-temperature model.

The results for the mole fractions of molecular and atomic nitrogen are shown in Fig. 6. As expected from the previous

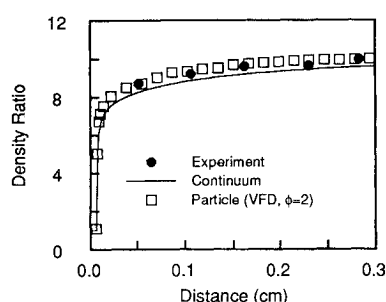


Fig. 4 Comparison of continuum and particle solutions of the local to upstream density ratio for case 2.

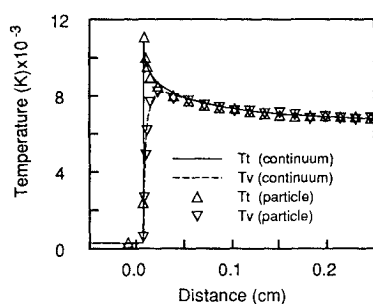


Fig. 5 Comparison of continuum and particle solutions of the translational and vibrational temperatures for case 2.

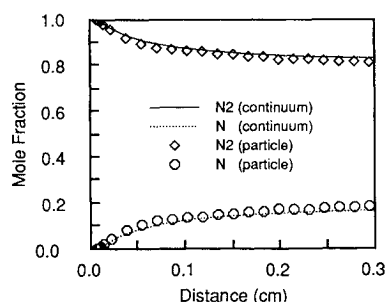


Fig. 6 Comparison of continuum and particle solutions of the species mole fractions for case 2.

comparisons, there is close agreement between the two numerical approaches with DSMC predicting slightly more dissociation than is obtained in the continuum solution.

Case 3: Strongly Dissociating Flow

The further increase in enthalpy for case 3 gives rise to stronger dissociation effects. Once again, the flow conditions modeled match those considered experimentally by Kewley and Hornung.²² The experimental profile of density behind the shock is compared with the computational results in Fig. 7. The comparison between the continuum solution and the experimental data is excellent. The DSMC profile is computed using the variable ζ_v model and $\phi = 2$. With this model configuration, the particle method provides excellent agreement with both the experiment and the continuum solution. It should be noted that this is the DSMC model configuration employed in the computations for case 2.

The translational and vibrational temperature profiles computed with the continuum and DSMC techniques are shown in Fig. 8. Generally, very good agreement is observed between the two. There is a noticeable difference in the peak vibrational temperatures computed by the two methods. This has quite significant implications for the estimation of radiative emission in such flows. The difference is attributable to dissociation-vibration coupling, i.e., how the vibrational energy distribution is affected by dissociation. This process is modeled quite differently in the continuum and particle approaches. These results indicate the need for experimental measurement of vibrational temperature profiles behind shock waves under conditions similar to those considered here. For completeness, the profiles of mole fractions of the neutral species are shown in Fig. 9. The stronger degree of dissociation for these flow conditions is very evident and, as expected, very good agreement is found between the two solutions.

For this strongly dissociating case, it is found that Park's two-temperature model reproduces the experimental data very well. It is very encouraging that the two-temperature model gives such a favorable comparison with the experimental data in strongly dissociating flow as this is the regime for which the model has been developed. Indeed, the present comparison arguably provides the strongest evidence to date that, despite its weak theoretical basis, the two-temperature model

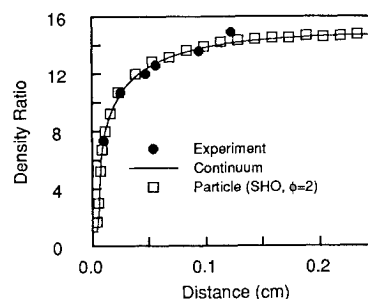


Fig. 7 Comparison of continuum and particle solutions of the local to upstream density ratio for case 3.

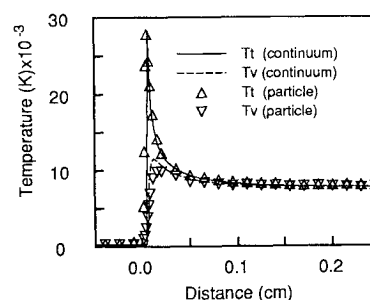


Fig. 8 Comparison of continuum and particle solutions of the translational and vibrational temperatures for case 3.

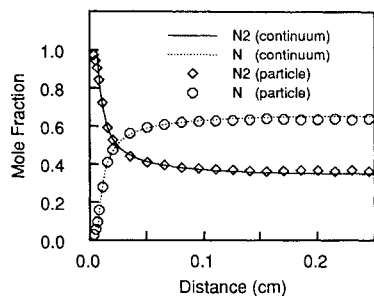


Fig. 9 Comparison of continuum and particle solutions of the species mole fractions for case 3.

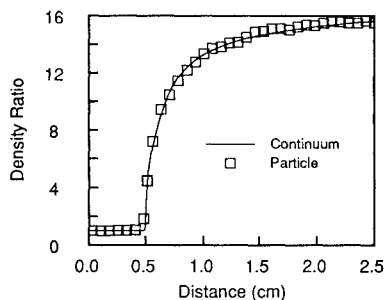


Fig. 10 Comparison of continuum and particle solutions of the local upstream density ratio for case 4.

does produce adequate simulation of strongly coupled vibration-dissociation processes. The present investigation is unique in that evaluation of the model is performed through direct comparison with experimental measurements of a fundamental flow quantity. The model was previously calibrated against experimental data by Park¹ through comparison with radiation emission spectra, and by Candler²³ through comparison with shock standoff distance. Due to the excellent comparisons between DSMC and experiment in Figs. 4 and 7, it is recommended that McDonald's collision mechanics and the VFD model with $\phi = 2$ be used for simulating nitrogen dissociation with the particle method.

Case 4: Weakly Ionizing Flow

The increase in enthalpy for case 4 is sufficient to give rise to significant ionization effects behind the shock. In performing the DSMC computations of the ionized flowfield, a steady-shock solution is first obtained with the ionizing reactions omitted. After reaching this point, the ionized species are included, and a further short transient phase in the simulation then allowed before sampling of flow properties is commenced. These procedures are adopted because the inclusion of electrons in the flowfield requires a reduction in computational time-step by two orders of magnitude. To compute the entire flowfield with such a small time-step would require much larger computational resources. The comparison for density profiles computed with the numerical techniques is shown in Fig. 10. As with the previous case, good agreement is obtained between the two solutions. The temperature profiles computed with the continuum and particle methods for the translational and vibrational modes are compared in Fig. 11. The peak values for each energy mode are in good agreement. It is observed that the translational temperature shock computed with DSMC is thicker than the continuum result. This is due to the relatively low upstream density employed in this investigation. A more thorough analysis of such behavior will form the basis of future study. The computed variations in mole fractions for the neutral species obtained with the numerical techniques are compared in Fig. 12 and those for the charged species are compared in Fig. 13. The agreement which is generally obtained is very satisfactory. This comparison verifies that the new forms of the reverse

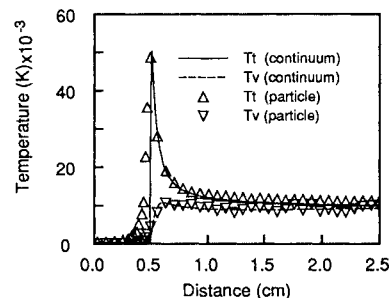


Fig. 11 Comparison of continuum and particle solutions of the translational and vibrational temperatures for case 4.

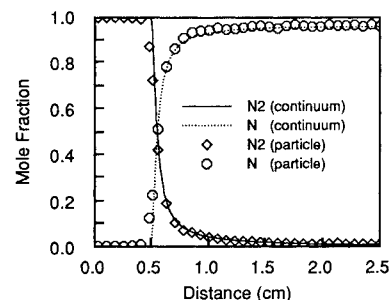


Fig. 12 Comparison of continuum and particle solutions of the neutral species mole fractions for case 4.

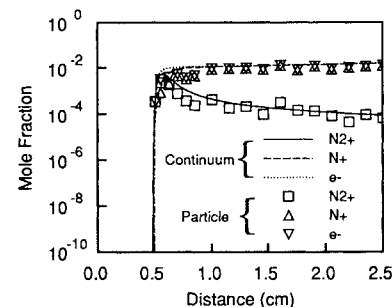


Fig. 13 Charged species mole fractions for case 4: particle simulation employed new chemical rate data.

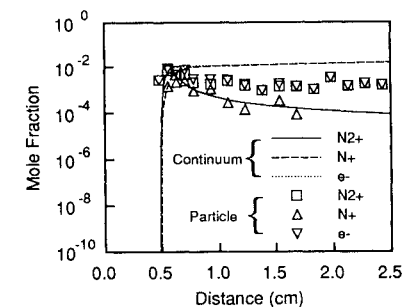


Fig. 14 Charged species mole fractions for case 4: particle simulation employed old chemical rate data.

reaction rates employed in the particle simulation are nearly equivalent to the expressions used in the continuum analysis. It should be noted that a degree of statistical scatter is exhibited by the DSMC results for the less abundant species.

To assess the effect of using the new reaction rates, a particle simulation is also performed with the rate data used by Bird.¹⁹ The variation in the mole fractions of the charged species computed in this way are compared with the continuum results in Fig. 14. None of the species profiles are found to be in good agreement. With Bird's rates, the most populous ion is N_2^+ , whereas the new particle rate data agrees with the continuum solution in giving N^+ as the most abundant ion. With Bird's rate data, the mole fraction of electrons at the downstream boundary is about 2.5×10^{-3} , whereas the con-

tinuum simulation gives a value of about 1.8×10^{-2} . If it is accepted that the rate coefficients provided in Refs. 1 and 2 are the more physically realistic, these large differences observed with Bird's older data set must call into question previous DSMC investigations which employed those reaction rates. As mentioned earlier, there has been a mistake in the reverse rate for reaction 3 used by Bird.¹⁹ The temperature exponent should be listed as -0.18 instead of the value of -0.52 .²⁰ This error is quite serious as it was included in codes employed in a fairly large number of studies.

Concluding Remarks

This study was motivated by the requirement to evaluate the relationship between continuum and particle simulations of hypersonic flows in the near-continuum regime. The results obtained in the investigation have established that a close correspondence exists between the thermochemical nonequilibrium models employed in these solution techniques. In the case of vibrational nonequilibrium, the agreement between the two sets of numerical results validated a number of recent modeling developments for computing the rate and mechanics of vibrational energy exchange in the particle simulation. In the cases of weak and strong dissociation, both the continuum and particle models for vibration-dissociation coupling were successfully evaluated against experimental data. This is a most interesting result, considering the large differences in the dissociation models employed in the two techniques. In the case of weakly ionized flow, it was necessary to develop new forms for some of the chemical rate constants for use in the particle simulation. These were developed so as to be nearly consistent with the continuum expressions, and also to be mathematically convenient for use in the particle chemistry models. The next stage in this continuing investigation will be the evaluation of these methods for flow conditions in the transition regime, i.e., at higher Knudsen numbers. In such flows, rarefaction effects may invalidate use of the Navier-Stokes equations, and give rise to large differences between the continuum and particle simulation results.

Acknowledgments

Support by NASA for I. D. Boyd, Grant NCC2-582, and for T. Gökçen, Grant NCC2-420, is gratefully acknowledged.

References

- ¹Park, C., *Nonequilibrium Hypersonic Aerothermodynamics*, Wiley, New York, 1989.
- ²Park, C., Howe, J. T., Jaffe, R. L., and Candler, G. V., "Chemical-Kinetic Problems of Future NASA Missions," AIAA Paper 91-0464, Jan. 1991.
- ³Millikan, R. C., and White, D. R., "Systematics of Vibrational Relaxation," *Journal of Chemical Physics*, Vol. 39, No. 12, 1963, pp. 3209-3213.
- ⁴MacCormack, R. W., "Current Status of the Numerical Solutions of the Navier-Stokes Equations," AIAA Paper 85-0032, Jan. 1985.
- ⁵Candler, G. V., "The Computation of Weakly Ionized Hypersonic Flows in Thermo-Chemical Nonequilibrium," Ph.D. Dissertation, Stanford Univ., Stanford, CA, 1988.
- ⁶Gökçen, T., "Computation of Hypersonic Low Density Flows with Thermochemical Nonequilibrium," Ph.D. Dissertation, Stanford Univ., Stanford, CA, 1989.
- ⁷Boyd, I. D., "Vectorization of a Monte Carlo Method for Nonequilibrium Gas Dynamics," *Journal of Computational Physics*, Vol. 96, No. 2, 1991, pp. 411-427.
- ⁸Boyd, I. D., "Analysis of Vibration-Dissociation-Recombination Processes Behind Strong Shock Waves of Nitrogen," *Physics of Fluids A*, Vol. 4, No. 1, 1992, pp. 178-185.
- ⁹Boyd, I. D., "Analysis of Rotational Nonequilibrium in Standing Shock Waves of Nitrogen," *AIAA Journal*, Vol. 28, No. 11, 1990, pp. 1997-1999.
- ¹⁰Borgnakke, C., and Larsen, P. S., "Statistical Collision Model for Monte Carlo Simulation of Polyatomic Gas Mixtures," *Journal of Computational Physics*, Vol. 18, 1975, pp. 405-420.
- ¹¹Boyd, I. D., "Rotational and Vibrational Nonequilibrium Effects in Rarefied Hypersonic Flow," *Journal of Thermophysics and Heat Transfer*, Vol. 4, No. 4, 1990, pp. 478-484.
- ¹²McDonald, J. D., "A Computationally Efficient Particle Simulation Method Suited to Vector Computer Architectures," Ph.D. Dissertation, Stanford Univ., Stanford, CA, 1990.
- ¹³Lumpkin, F. E., Haas, B. L., and Boyd, I. D., "Resolution of Differences Between Collision Number Definitions in Particle and Continuum Simulations," *Physics of Fluids A*, Vol. 3, No. 9, 1991, pp. 2282-2284.
- ¹⁴Haas, B. L., and Boyd, I. D., "Models for Vibrationally-Favored Dissociation Applicable to a Particle Simulation," AIAA Paper 91-0774, Jan. 1991.
- ¹⁵Bird, G. A., "Simulation of Multi-Dimensional and Chemically Reacting Flows," *Rarefied Gas Dynamics*, edited by R. Campargue, CEA, Paris, 1979, pp. 365-388.
- ¹⁶Boyd, I. D., and Whiting, E. E., "Decoupled Predictions of Radiative Heating in Air Using a Particle Simulation Method," AIAA Paper 92-2971, July 1992.
- ¹⁷Byron, S., "Shock-Tube Measurement of the Rate of Dissociation of Nitrogen," *Journal of Chemical Physics*, Vol. 44, Feb. 1966, pp. 1378-1388.
- ¹⁸Mitcheltree, R. A., "A Parametric Study of Dissociation and Ionization at 12 km/sec," AIAA Paper 91-1368, June 1991.
- ¹⁹Bird, G. A., "Nonequilibrium Radiation During Re-Entry at 10 km/s," AIAA Paper 87-1543, June 1987.
- ²⁰Bird, G. A., private communication, Killara, Australia, July 1992.
- ²¹Boyd, I. D., and Stark, J. P. W., "Direct Simulation of Chemical Reactions," *Journal of Thermophysics and Heat Transfer*, Vol. 4, No. 3, 1990, pp. 391-393.
- ²²Kewley, D. J., and Hornung, H. G., "Free-Piston Shock-Tube Study of Nitrogen Dissociation," *Chemical Physics Letters*, Vol. 25, No. 4, 1974, pp. 531-536.
- ²³Candler, G. V., "On the Computation of Shock Shapes in Nonequilibrium Hypersonic Flows," AIAA Paper 89-0312, Jan. 1989.